

## Article

# Integrated Proteomic and Metabolomic Analysis of Cassava cv. Kasetsart 50 Infected with *Sri Lankan Cassava Mosaic Virus*

Wanwisa Siriwan <sup>1</sup>, Nattachai Vannatim <sup>1</sup>, Somruthai Chaowongdee <sup>2,3</sup>, Sittiruk Roytrakul <sup>4</sup>, Sawanya Charoenlapanit <sup>4</sup>, Pornkanok Pongpamorn <sup>5</sup>, Atchara Paemaneer <sup>5</sup> and Srihunsu Malichan <sup>1,\*</sup>

<sup>1</sup> Department of Plant Pathology, Faculty of Agriculture, Kasetsart University, Bangkok 10900, Thailand; wanwisa.si@ku.th (W.S.)

<sup>2</sup> Center of Excellence on Agricultural Biotechnology (AG-BIO/MHESI), Bangkok 10900, Thailand

<sup>3</sup> Center for Agricultural Biotechnology, Kasetsart University, Kamphaeng Saen Campus, Nakhon Pathom 73140, Thailand

<sup>4</sup> National Center for Genetic and Engineering and Biotechnology (BIOTEC), National Science and Technology Development Agency, Pathum Thani 12120, Thailand

<sup>5</sup> National Omics Center (NOC), National Science and Technology Development Agency (NSTDA), Pathum Thani 12120, Thailand

\* Correspondence: fagrsm@ku.ac.th; Tel.: +662-579-1026

**Abstract:** Cassava mosaic disease (CMD) is a major disease affecting cassava production in Southeast Asia. This study aimed to perform an integrated proteomics and metabolomics analysis of cassava cv. Kasetsart 50 infected with *Sri Lankan cassava mosaic virus* (SLCMV). Proteomics analyses revealed that 359 proteins were enriched in the plant–pathogen interaction, plant hormone signal transduction, and MAPK signaling pathways. A total of 79 compounds were identified by metabolomics analysis of the healthy and SLCMV-infected cassava plants. Integrated omics analysis revealed that 9 proteins and 5 metabolites were enriched in 11 KEGG pathways. The metabolic pathways, plant hormone signal transduction, and plant–pathogen interaction pathway terms were specifically investigated. The findings revealed that caffeic acid and chlorogenic acid were associated with the plant–pathogen interaction pathway, histidine (HK3) was involved in plant hormone signal transduction, while citric acid and D-serine were associated with the metabolic pathways. KEGG functional enrichment analysis revealed that plant–pathogen interaction, plant hormone signal transduction, and metabolic pathways were linked via the enriched protein (protein phosphatase 2C) and metabolites (cyclic nucleotide-binding (AT2G20050) and D-serine). The available information and resources for proteomics and metabolomics analyses of cassava can elucidate the mechanism of disease resistance and aid in cassava crop improvement programs.

**Keywords:** proteomics; metabolomics; cassava mosaic disease; Kasetsart 50; metabolic pathways; plant hormone signal transduction; plant–pathogen interaction



**Citation:** Siriwan, W.; Vannatim, N.; Chaowongdee, S.; Roytrakul, S.; Charoenlapanit, S.; Pongpamorn, P.; Paemaneer, A.; Malichan, S.

Integrated Proteomic and Metabolomic Analysis of Cassava cv. Kasetsart 50 Infected with *Sri Lankan Cassava Mosaic Virus*. *Agronomy* **2023**, *13*, 945. <https://doi.org/10.3390/agronomy13030945>

Academic Editors: Guoliang Li, Xiaoxi Meng and Desalegn D. Serba

Received: 26 January 2023

Revised: 14 March 2023

Accepted: 16 March 2023

Published: 22 March 2023



**Copyright:** © 2023 by the authors. Licensee MDPI, Basel, Switzerland. This article is an open access article distributed under the terms and conditions of the Creative Commons Attribution (CC BY) license (<https://creativecommons.org/licenses/by/4.0/>).

## 1. Introduction

Cassava mosaic disease (CMD) poses a serious threat to the cassava industry in Southeast Asian countries, including Cambodia [1], Vietnam [2], Thailand [3], and Laos [4]. CMD can significantly decrease the yield of cassava by up to 50% or more in susceptible varieties of cassava [5]. The Kasetsart 50 (KU50) cassava variety has gained popularity among farmers since its availability in 1992 [6]. Apart from its high starch content and excellent yield, the KU50 variety exhibits tolerance to CMD in greenhouses and naturally infected fields [5,7]. Current practices are encouraging the replacement of CMD-susceptible varieties with KU50 for developing resistance varieties that would aid in preventing the spread of CMD in the region. In Southeast Asia, CMD is caused by the *Sri Lankan cassava mosaic virus* (SLCMV), which belongs to the *Begomovirus* genus under the *Geminiviridae* family. The virus was first reported in Cambodia in 2015 [1] and spread rapidly thereafter

via infected stem cuttings [8]. SLCMV can also be transmitted by whiteflies (*Bemisia tabaci*), especially those of the Asia II-1 biotype [9,10].

Plants need to develop dynamic constitutive, and inducible defense mechanisms in response to biotic stresses, including pathogen invasions. The initial line of plant defense comprises constitutive defense mechanisms, including cell walls, waxy substances, cuticles, and bark. The stimulated defense mechanisms include pathogen-associated molecular pattern (PAMP)-triggered immunity (PTI) and effector-triggered immunity (ETI) [11]. The “zigzag” model proposed in an earlier study describes the plant defense mechanisms [12]. In particular, reactive oxygen species (ROS) and hormone activation are linked to complex signaling cascade networks and regulate kinase signals for inducing the expression of defense-related genes via transcription factors (TFs). These genes induce the production of various secondary metabolites and antimicrobial compounds, including phytoalexins and phenolics, among others [13].

Proteins and metabolites are involved in the last step of genomic regulation and play key roles in fundamental life processes. The proteins involved in plant defense mechanisms include (1) phytohormones, ROS, and pathogenesis-related (PR) proteins; (2) TFs and post-transcriptional factors; and (3) protein receptors [14]. The metabolites produced by plants have precise molecular functions. Erb and Kliebenstein [15] described hundreds of thousands of organic compounds produced by the plant kingdom. They classified the compounds based on perspective function into primary metabolites, secondary metabolites, and plant hormones.

The present study aimed to perform a comprehensive proteomics and metabolomics analysis of cassava plants with CMD to determine the alterations in regulating protein abundance and metabolites. The findings of this study provide novel insights for further studies on the mechanism underlying the resistance of cassava to SLCMV. In addition, the results would also aid in establishing the plant defense response network of cassava and identifying the candidate proteins and metabolites for selecting the SLCMV-resistance variety of cassava.

## 2. Materials and Methods

### 2.1. Plant Materials

In this study, the stems of cassava cv. KU50 were used for vegetative propagation in both the SLCMV-infected and uninfected healthy groups. All the plant materials were provided by the Thai Tapioca Development Institute (TTDI), Nakhon Ratchasima, Thailand. The stems, containing 3–4 buds each, were cut into 15 cm-long segments and planted in plastic pots with a diameter of 20 cm in the greenhouse of the Department of Plant Pathology, Faculty of Kasetsart University, Thailand. After 45 days of cultivation, the apices of the healthy and diseased stems were collected, and the leaves from the stems of three different plants were combined into a single sample. The leaves were immediately flash-frozen in liquid nitrogen to cease all metabolic activity. The frozen samples were kept at  $-80\text{ }^{\circ}\text{C}$  until the extraction of proteins and metabolites in the subsequent steps.

The phenotypes of the leaves of infected and healthy cassava cv. KU50 plants were observed after 14 days of planting. The samples of leaves were collected for DNA extraction. The DNA was extracted from 200 mg of ground cassava leaf powder using the CTAB method [16]. The DNA was resuspended in ddH<sub>2</sub>O containing 100  $\mu\text{g}/\text{mL}$  RNase (Thermo Fisher Scientific, Waltham, MA, USA) and stored at  $-20\text{ }^{\circ}\text{C}$ . The quantity and integrity of the DNA samples were determined by agarose gel electrophoresis and a Nanodrop spectrophotometer (NanoDrop Technologies, Thermo Scientific), respectively.

The *AV1* gene of SLCMV was amplified by polymerase chain reaction (PCR) using the following gene-specific primers: 5'-GTTGAAGGTTACTTATTCCC-3' (forward) and 5'-TATTAATACGGTGTAAACGC-3' (reverse) [9]. Approximately 50 ng of the genomic DNA, 0.2 M of each of the forward and reverse primers, and 1XPCR buffer (PCR Biosystems, London, UK) were used for amplification. The conditions of PCR amplification were as follows: initial denaturation at  $94\text{ }^{\circ}\text{C}$  for 5 min, followed by 35 cycles of denaturation

at 94 °C for 40 s, annealing at 55 °C for 40 s, and elongation at 72 °C for 40 s. The final elongation was performed at 72 °C for 5 min. The amplified products were analyzed by gel electrophoresis using 1.5% agarose TAE gels containing RedSafe Nucleic Acid Staining Solution (iNtRON Biotechnology, Sangdaewon, Republic of Korea) and compared with those of the positive control.

## 2.2. Protein Extraction and Liquid Chromatography-Tandem Mass Spectrometry (LC/MS-MS)

For protein extraction, 100 mg of each sample's fine cassava tissue powder was resuspended with 1 mL 0.5% sodium dodecyl sulfate (SDS) and mixed in a vortex mixer for 1 h, following which the extraction tube was centrifuged at  $9000\times g$  for 15 min. The supernatant was transferred to a new tube, and 1400  $\mu\text{L}$  of cold acetone was added to precipitate the proteins. The mixture was incubated overnight at  $-20\text{ }^{\circ}\text{C}$ . The mixture of proteins was centrifuged at  $9000\times g$  for 15 min, and the supernatant was discarded. The protein pellet was dried and stored at  $-80\text{ }^{\circ}\text{C}$ . The pellets were resuspended in 0.5% SDS. The Lowry method was used to determine the concentration of the proteins [17]. The absorbance was measured at 750 nm ( $\text{OD}_{750}$ ), and the concentration of the proteins was determined using a standard curve established using a serial dilution of bovine serum albumin (BSA).

A 5- $\mu\text{g}$  sample of the total protein was subjected to in-solution protease digestion. Briefly, 10 mM ammonium bicarbonate (AMBIC) buffer was used for dissolving the samples. Dithiothreitol (DTT) was added to a final concentration of 5 mM, and the solution was subsequently incubated at  $60\text{ }^{\circ}\text{C}$  for 1 h to reduce the disulfide bonds. The sulfhydryl groups were finally alkylated by incubating with AMBIC buffer containing 15 mM iodoacetamide for 45 min at  $26\text{ }^{\circ}\text{C}$  in the dark. The protein was subsequently digested, following which the samples were mixed with 50 ng/ $\mu\text{L}$  of sequencing grade trypsin at a ratio of 1:20 (Promega, Fitchburg, WI, USA) and incubated overnight at  $37\text{ }^{\circ}\text{C}$ . The digested samples were dried and protonated with 0.1% formic acid before LC-MS/MS analysis.

The digested samples were prepared for injecting into an Ultimate3000 Nano/Capillary LC System (Thermo Scientific) coupled to a Hybrid quadrupole Q-ToF impact II<sup>TM</sup> (Bruker Daltonics, Billerica, MA, USA) equipped with a Nano-captive spray ion source. Briefly, 1  $\mu\text{L}$  of the digested peptide was enriched on a  $\mu$ -Precolumn 300  $\mu\text{m}$  i.d.  $\times$  5 mm C18 Pepmap 100, 5  $\mu\text{m}$ , 100 A (Thermo Scientific, Massachusetts, UK), separated on a 75- $\mu\text{m}$  I.D.  $\times$  15 cm column packed with Acclaim PepMap RSLC C18, 2  $\mu\text{m}$ , 100  $\text{\AA}$ , nanoViper (Thermo Scientific). The C18 column was enclosed in a thermostatic column oven at a temperature of  $60\text{ }^{\circ}\text{C}$ . Solvent A comprised 0.1% formic acid in the water, and solvent B comprised 0.1% formic acid in 80% acetonitrile. The peptides were eluted with a 5–55% gradient of solvent B at a constant flow rate of 0.30  $\mu\text{L}/\text{min}$  for 30 min. Electrospray ionization was performed at 1.6 kV using CaptiveSpray. Nitrogen was used as the drying gas, and the flow rate was approximately 50 L/h. The collision-induced-dissociation (CID) product ion mass spectra were obtained using nitrogen as the collision gas. The mass spectra and MS/MS spectra were obtained in the positive-ion mode at 2 Hz over a range of 150–2200  $m/z$ . The collision energy was adjusted to 10 eV as a function of the value of  $m/z$ . LC-MS analysis of each sample was performed in triplicate.

## 2.3. Analysis of Proteomic Data

The MaxQuant software package, version 2.0.3.0, and the Andromeda search engine were used for quantitating the proteins in the individual samples. The peptide fragments were identified by comparing the MS/MS spectra to the *Manihot esculenta* dataset in UniProt Knowledgebase. Label-free quantitation was performed using the default setting in MaxQuant, in which the maximum number of miss-cleavage sites was set to 2, and the mass tolerance was set to 0.6 Dalton for the main search. During the search, trypsin was selected as the digesting enzyme, cysteine carbamidomethylation was selected as a fixed modification, and the oxidation of methionine and acetylation of the N-termini of proteins were selected as variable modifications. The peptide peaks that contained a

minimum of seven amino acids and representing a single sequence motif were selected for further analyses. Protein identification depended on whether at least two corresponding peptides were detected, of which at least one was unique. The proteins that satisfied these criteria were selected for data analysis. The false discovery rate (FDR) was set at 1% and was determined using the reversed search sequences. The maximum number of modifications for any given peptide was set to 5. The FASTA sequences of the proteins in the *M. esculenta* proteome were retrieved from the UniProt database. The potential contaminants in the contaminant FASTA file provided with the MaxQuant software were automatically added to the search space. The MaxQuant ProteinGroups.txt file was loaded into the Perseus search platform, version 1.6.6.0 [18], and the potential outliers that did not correspond to any Universal Proteomics Standard Set 1 (UPS1) protein were removed from the dataset. The maximum intensities were log<sub>2</sub>-transformed, and the pairwise comparisons were performed with *t*-tests. The missing values were also imputed in Perseus using a constant value of 0. Data visualization and statistical analyses were conducted using the MultiExperiment Viewer (MeV) module of the TM4 software suite [19]. The organization and biological functions of the proteins were determined using protein analysis through the evolutionary relationships (Panther) protein classification database [20].

#### 2.4. Metabolite Profiling by UHPLC-HRMS/MS

The metabolites were extracted from 100 mg of fresh cassava leaves in each sample group. The leaves were ground to a fine powder, and 750 µL extraction buffer (75% methanol, 20% water, and 5% formic acid (FA)) was added. The mixture of samples was vortexed for 30 s and incubated on ice for 10 min. The tubes containing the mixture were centrifuged at 1500 × *g* for 5 min. The supernatant was subsequently transferred to a clean tube, and the pellets were subjected to the extraction process, which was repeated twice. The supernatants from each sample were combined and dried using a centrifugal concentrator.

Approximately 200 ppm of cassava metabolite extraction solution was separated on a Hypersil GOLD™ Vanquish C18 column (2.1 × 100 mm, 1.9 µm, Thermo Scientific) with a guard column at a temperature of 40 °C and a flow rate of 0.4 mL/min. Mobile phase A comprised 0.1% FA in water, and mobile phase B comprised 0.1% FA in acetonitrile. After 4 min of elution with 5% B, the percentage of phase B was increased to 90% over 10 min. Next, the column was flushed with 90% B for 4 min, following which the concentration of phase B was decreased to 5% over a duration of 1 min before returning to the initial conditions for 25 min.

MS acquisition was performed with a Q-Exactive HF-X Orbitrap mass spectrophotometer (Thermo Scientific) and a heated electrospray ionization (HESI) ion source. The negative and positive ions were detected using the full-scan MS1/data-dependent MS2 (dd-MS2) mode, with the following settings: spray voltage: 3.5 kV (positive) and 2.5 kV (negative); sheath gas: 45 AU; auxiliary gas: 10 AU; sweep gas: 2 AU; capillary temperature: 250 °C; full-scan MS1 resolution: 120,000; data-dependent MS2 resolution: 30,000; scan range: 100–1500 *m/z*; automatic gain control target: 3e6; maximum injection time: 100 ms; and stepped N(CE): 20, 30, 40 eV. The acquired files were processed using the Compound Discoverer software, and the compounds were annotated with the mzCloud, mzVault, and ChemSpider databases.

#### 2.5. Statistical Analysis and Identification of Metabolites

Statistical analysis of the infected and healthy cassava plant datasets was performed with MetaboAnalyst software, version 4.0 [21]. The data were log-transformed and pareto scaled for subsequent analyses. The phenotypes of the healthy uninfected plants were compared to those of the virus-infected plants based on the relative abundance of the metabolites. Principal component analysis (PCA) of the infected and healthy cassava plants was performed. The data were analyzed to identify the metabolites that can be used to differentiate between infected and healthy samples. Fold Change analysis, *t*-tests, and volcano plots were used to compare the data from the healthy and infected plant groups.

The potential metabolites were identified by one-way analysis of variance (ANOVA), followed by post-hoc analysis and correlation analysis. A heatmap was generated based on the Euclidean distances, and Pearson's correlation and Spearman's rank correlation were also performed. Enrichment analysis was performed with the Kyoto Encyclopedia of Genes and Genomes (KEGG) metabolic pathway database [22].

### 2.6. Integrated Proteomics and Metabolomics Analysis

The functions and pathways of the differentially expressed proteins and metabolites were determined using the KEGG mapper reconstruction pathway analysis tool (<https://www.kegg.jp/blastkoala/> accessed on 15 December 2021) and the *M. esculenta* (cassava) proteome dataset, which was annotated based on literature and PubChem data (<https://pubchem.ncbi.nlm.nih.gov/> accessed on 15 December 2021). A protein–protein interaction network was constructed using STRING, version 11.5, and STITCH, version 5.0 (<http://stitch.embl.de/> accessed on 20 December 2021) and used for mapping the interactions between the proteins and metabolites.

## 3. Results

### 3.1. Proteomics Analysis

A total of 1813 proteins were identified from the healthy and SLCMV-infected cassava plant samples in this study, of which 749 proteins were assigned to specific functions. The results demonstrated that 41.3% of the proteins of the healthy and SLCMV-infected cassava plants could be classified by KEGG functional category analysis. Of these, 359 proteins were identified from the SLCMV-infected plants, and 99.7% of the proteome were enriched in the genetic information processes, genetic information processing, and carbohydrate metabolism pathways, while the proteins were enriched in the metabolism, signaling and cellular processing, unclassified metabolism, energy metabolism, environmental information processing, lipid metabolism, cellular processes, and metabolism of terpenoid and polyketides terms. The functional categories of the proteome of SLCMV are depicted in Figure 1.

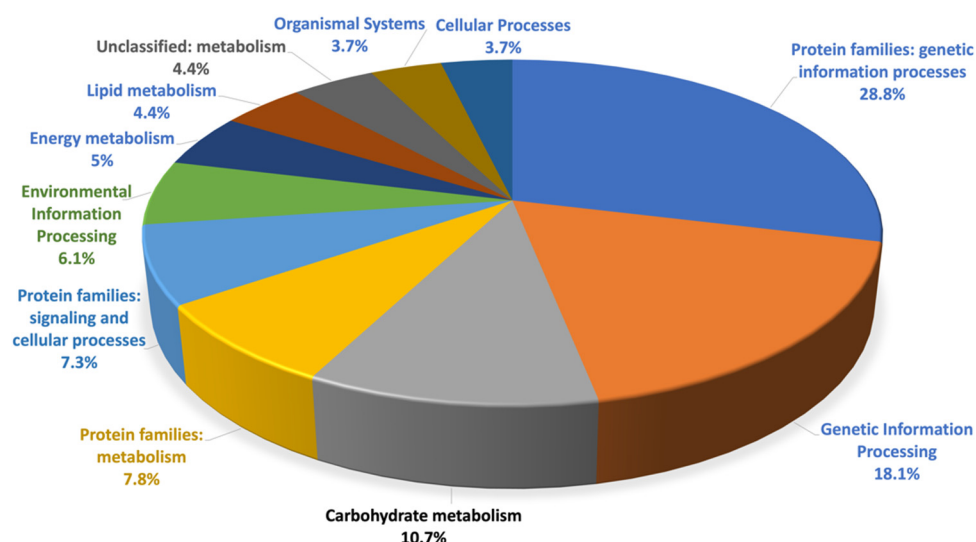


**Figure 1.** Functional classification of the differentially expressed proteins in the leaves of cassava cv. KU50 infected with SLCMV.

The protein–protein interaction network was constructed using STRING version 11.5. The proteins were represented by nodes, the associations between protein pairs were indicated by the edges, and the strength of the association between protein pairs was indicated by the length of each edge. The results of functional protein–protein interaction analysis revealed significant enrichment ( $p < 0.05$ ). The KEGG pathways of the upregulated proteins,



To investigate the mechanism of defense of cassava plants following infection with SLCMV, the proteins identified in the infected cassava plants were subjected to KEGG analysis. The proteomics data obtained in this study were compared to existing data, and four metabolic pathways were identified in SLCMV-infected plants that are known to activate proteins related to plant defense. These four metabolic pathways are discussed in detail hereafter. Analysis with the Reconstruct tool in KEGG Mapper revealed that the plant–pathogen interaction pathway was enriched during environmental adaptation (Figure 3). A total of six proteins, namely the cyclic nucleotide-binding domain-containing protein (CNGC; A0A2C9W0Z2), calcium-dependent protein kinase (CPK; A0A2C9V5W0), WRKY transcription factor 25 (WRKY25; A0A140H8T1), respiratory burst oxidase homolog (RBOH) protein A (RBOHA; A0A2C9WBJ4), calmodulin-like protein 1 (CALM1; A0A2C9WL80), and 3-ketoacyl-CoA synthase (KCS; A0A2C9W899), were significantly enriched in the plant–pathogen interaction term. In addition, enrichment analysis revealed that the cytokinin receptor (CRE1; A0A2C9UUG0), serine/threonine-protein kinase 2 (SnRK2; A0A251K1B9), and the regulatory protein NPR1 (A0A251KAS6) were significantly enriched in the plant hormone signal transduction pathway (Figure 4). In this pathway, the salicylic acid (SA) produced during the metabolism of phenylalanine activates NPR1, which is repressed in plants with the disease-resistant phenotype. The MAPK signaling pathway is a subcategory of the signal transduction pathway, and five proteins were enriched in the MAPK pathway, namely the WRKY TF 33 (WRKY33; A0A140H8T1), the RAN1 P-type Cu<sup>+</sup> transporter (A0A2C9WKV2), SnRK2 (A0A251K1B9), catalase (CAT; A9YME8), and RBOH (A0A2C9UA53) (Figure 5).

### 3.2. Metabolomics Analysis

The SLCMV-infected KU50 variety of cassava and the uninfected healthy cassava leaves were subjected to metabolomics analysis with UHPLC-HRMS/MS. A total of 79 features were identified from all the treatment groups, and the raw data were submitted to the ScienceDB database <https://www.scidb.cn/en/s/uAbEzq>; 15 December 2021. Comparison of the features of the healthy and SLCMV-infected cassava leaf samples with one-way ANOVA revealed that the majority of the metabolite features were significantly affected following SLCMV infection. The metabolite features were observed using heatmaps constructed by hierarchical clustering of their abundance values (Figure 6). Analysis of the metabolic profile revealed that some of the metabolite features of the SLCMV-infected plants had higher abundance values than those of the uninfected samples.

The differences between the metabolic profiles of the infected and healthy samples were compared based on the relative abundances of metabolite features (abundance in SLCMV-infected samples/abundance in uninfected samples). PCA of the abundance values revealed marked differences between the profiles of the metabolites in the infected and healthy samples (Figure 7). KEGG pathway enrichment analysis of the identified metabolite features was performed using the KEGG metabolic pathway database. The compounds identified in the infected and uninfected healthy plants were primarily enriched in aminoacyl-tRNA biosynthesis, followed by the valine, leucine, and isoleucine biosynthesis term, the alanine, aspartate and glutamate metabolism pathway, the phenylalanine, tyrosine, and tryptophan biosynthesis pathway, histidine metabolism, and starch and sucrose metabolism pathways (Figure 8).

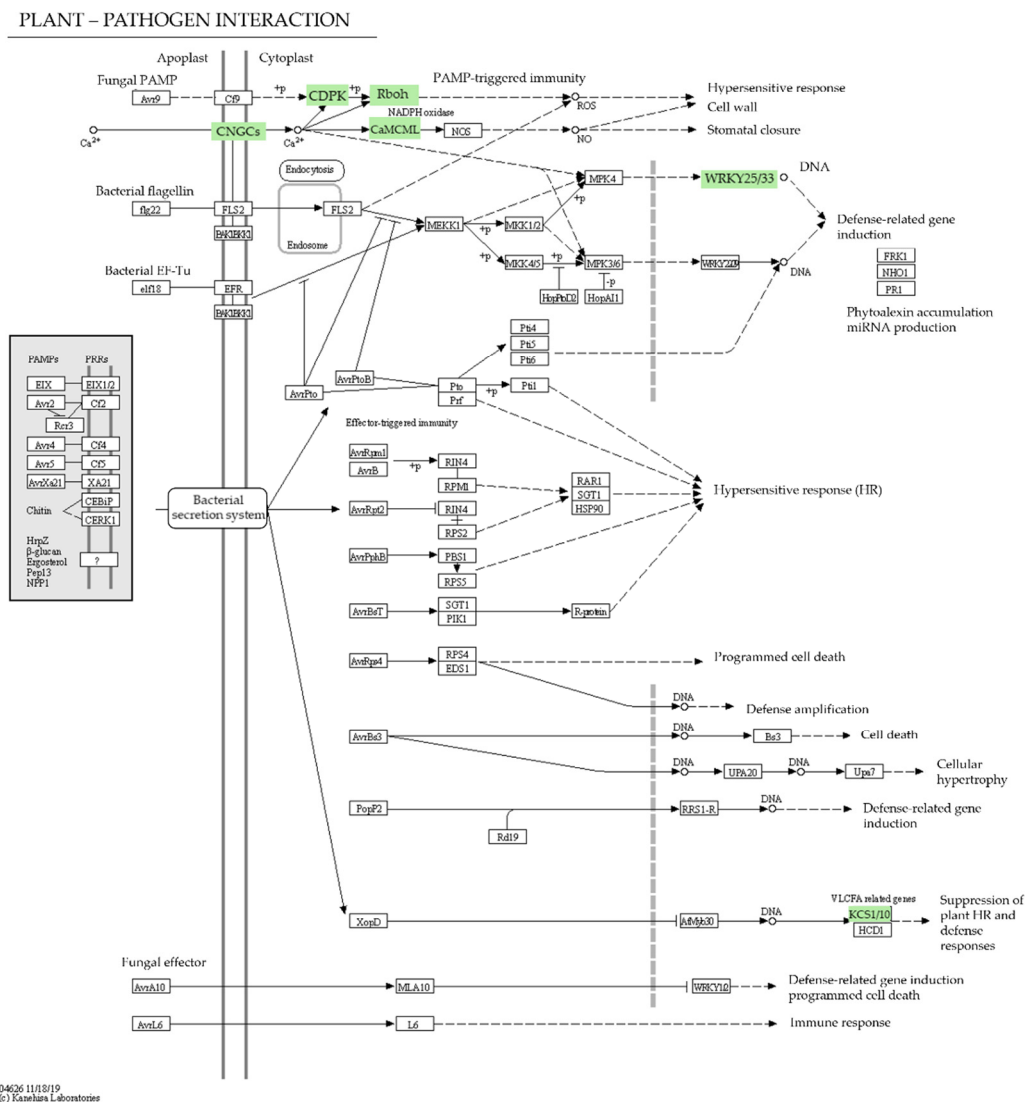


**Figure 3.** KEGG annotation and pathway mapping of the plant–pathogen interactions in cassava plants infected with SLCMV. The six proteins in the green boxes were identified by proteomics analysis and included the cyclic nucleotide-binding domain-containing protein (CNGC; A0A2C9W0Z2), calcium-dependent protein kinase (CPK; A0A2C9V5W0), WRKY TF 25 (WRKY25; A0A140H8T1), respiratory burst oxidase homolog protein A (RBOH; A0A2C9WBJ4), calmodulin-like protein 1 (CALM; A0A2C9WL80), and 3-ketoacyl-CoA synthase (KCS; A0A2C9W899).

Metabolite biomarkers were identified for constructing a predictive model of one or multiple metabolites to evaluate the performance or robustness of the model in classifying healthy and infected plants in future studies. A ROC curve of the characterized biomarkers was constructed for evaluating the performance of the biomarker models created based on the automated identification of import features with the MetaboAnalystR database. A total of 10 metabolite features were identified as biomarkers that could be used for predicting the infected and healthy cassava plants. Kaempferol-3-O-rutin, 4-hydroxybenzaldehyde, choline, trifolin, rhamnetin, myricetin, and robinetin were upregulated during SLCMV infection, while norfludiazepam, quercetin, and (-)-3-dehydroshikimi were upregulated in the leaves of healthy cassava plants (Figure 9).

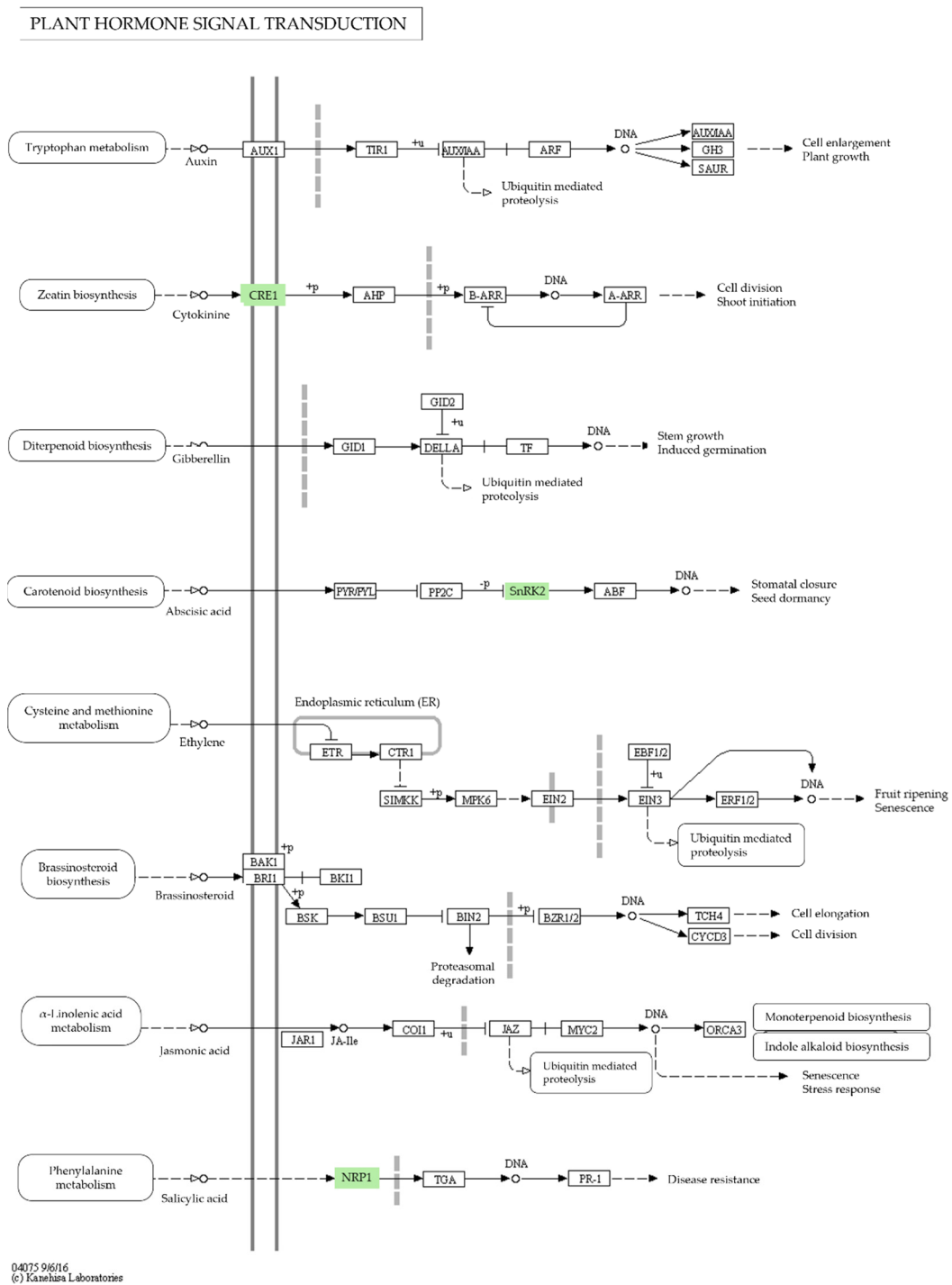


**Figure 4.** KEGG annotation and mapping of the plant hormone signal transduction pathways. Three proteins were identified from cassava plants infected with SLCMV and are highlighted in the green boxes. The proteins included the CRE1 cytokinin receptor (A0A2C9UUG0), serine/threonine-protein kinase 2 (SnRK2; A0A251K1B9), and the NRP1 regulatory protein (A0A251KAS6).

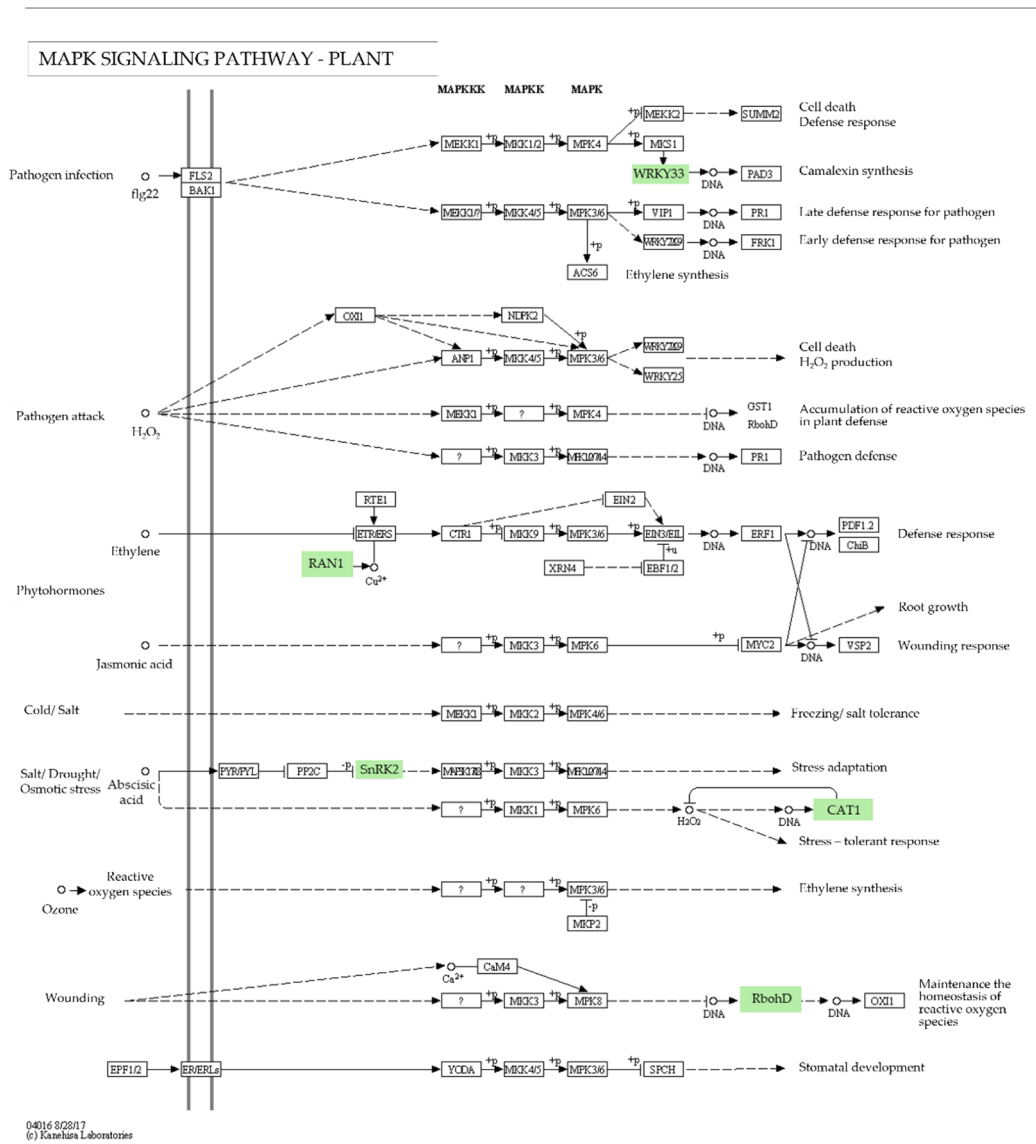


**Figure 5.** KEGG annotation and mapping of the proteins in the MAPK signaling pathway that were upregulated in cassava plants infected with SLCMV. These five proteins are indicated in the green boxes and include the WRKY TF 33 (WRKY33; A0A140H8T1), P-type Cu<sup>+</sup> transporter (RAN1; A0A2C9WKV2), SnRK2 (A0A251K1B9), catalase (CAT; A9YME8), and RBOH (A0A2C9UA53).

### 3.3. Integrated Proteomics and Metabolomics Analysis

The STITCH tool was used for the integrated analysis of the proteins and metabolites, and the interaction networks are depicted in Figure 10. The results of integrated proteomics and metabolomics analysis revealed that 9 proteins and 5 metabolites of infected cassava plants were enriched in 11 KEGG pathways, namely plant hormone signal transduction; microbial metabolism in diverse environments; glycine, serine, and threonine metabolism; biosynthesis of amino acids; plant–pathogen interaction; citrate cycle (TCA cycle); carbon metabolism; sulfur metabolism; cysteine and methionine metabolism; metabolic pathways; and biosynthesis of secondary metabolites. The findings revealed that several proteins in the infected samples were mostly enriched in the plant–pathogen interaction pathway, including WRKY25, WRKY33, calcium-dependent protein kinase 1 (CDPK1), RBOHA, and RBOHD.

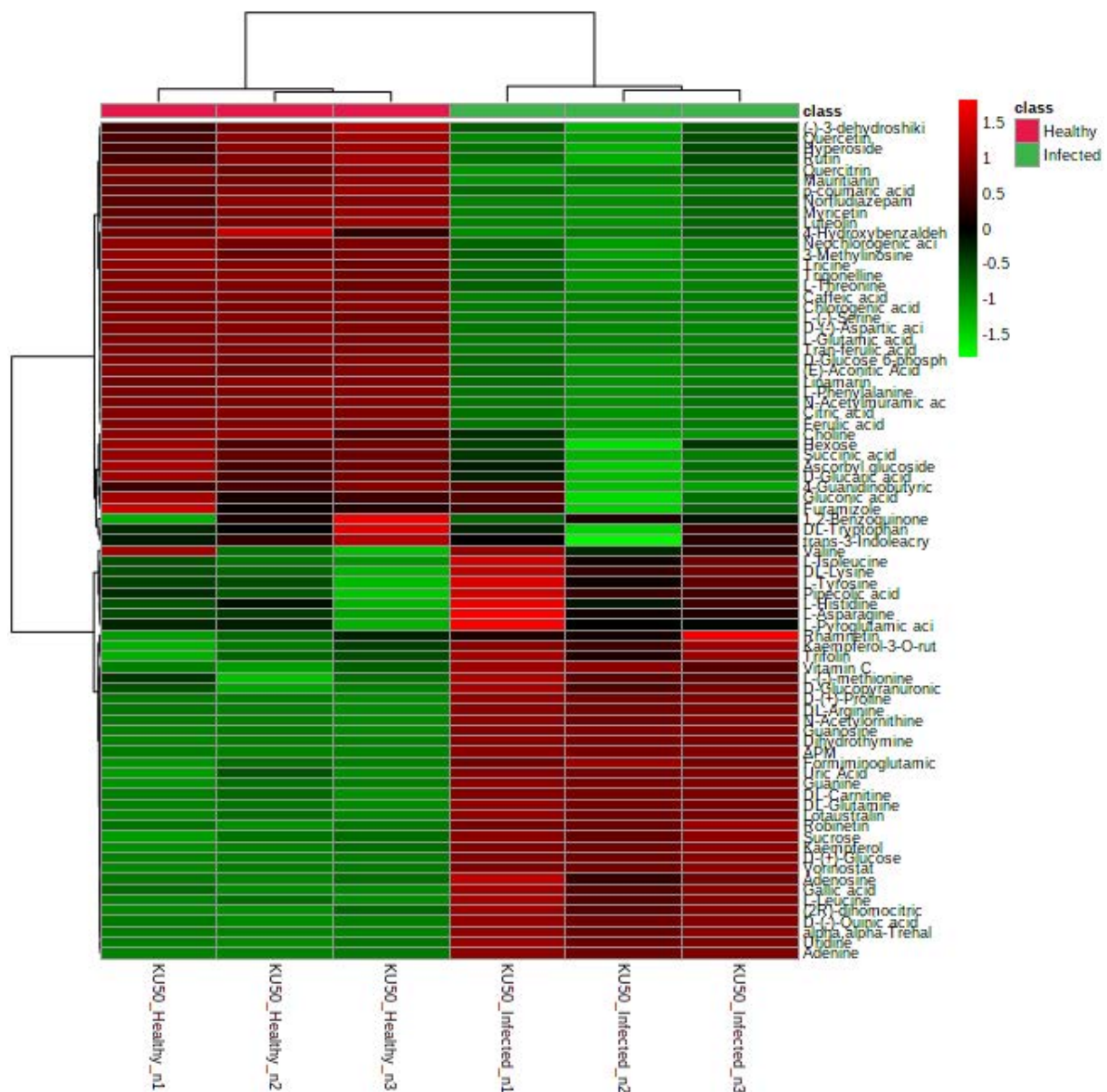


**Figure 6.** Comparison of the abundance of the metabolites of SLCMV–infected and uninfected KU50 cassava plants using a heatmap constructed by hierarchical clustering of the abundance values of the metabolites. The red and green bars depict healthy and SLCMV–infected cassava plants; the abundances of the metabolites are indicated by the colors of the bars, where dark red denotes high abundance and light green denotes low abundance.

This study focused on the plant–pathogen interaction pathway, plant hormone signal transduction, and metabolic pathways. The protein–metabolite interaction analyses were consistent with the results of proteomics analysis of the SLCMV-infected samples. However, the results shown in Figure 10 imply that caffeic acid and chlorogenic acid (CGA) were enriched in the plant–pathogen interaction pathway, histidine (HK3) was involved in plant hormone signal transduction, while citric acid and D-serine were enriched in the metabolic pathways. Functional enrichment analysis with KEGG indicated that the plant–pathogen interaction pathway, plant hormone signal transduction, and metabolic pathways were linked by the enriched protein (protein phosphatase 2C) and metabolites (cyclic nucleotide-binding (AT2G20050) and D-serine). These findings suggested that the expression of specific proteins and the accumulation of certain metabolites under conditions of biotic stress, and especially viral infections, regulates certain protein and metabolic pathways,

which leads to the generation of a plant defense mechanism against the invasion of the viral pathogen.

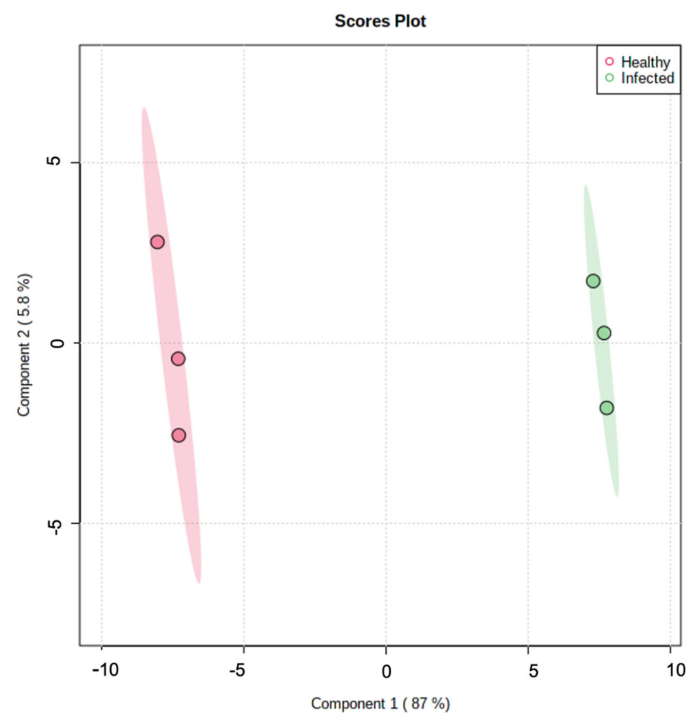


**Figure 7.** PCA plot depicting the differences between healthy and infected plant samples. PCA revealed considerable differences in the profiles of the metabolites that were differentially expressed in the infected and healthy samples. The green and pink dots denote infected and healthy cassava plants, respectively.

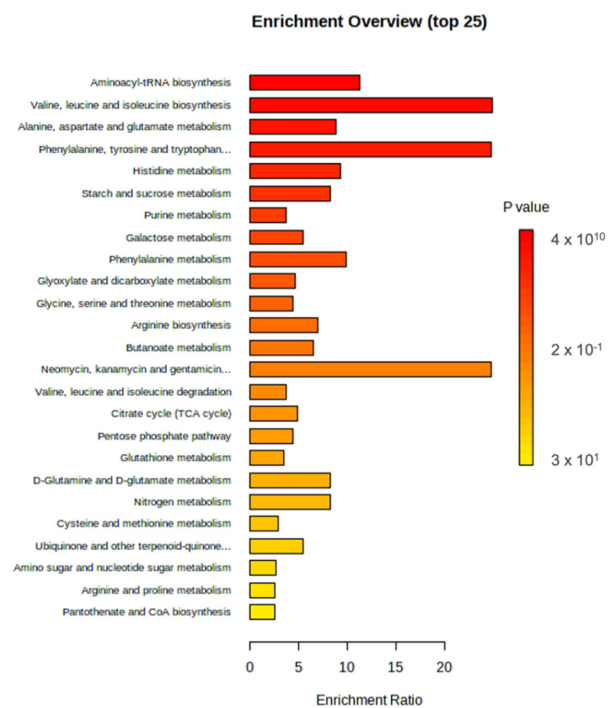


**Figure 8.** KEGG pathway enrichment analysis of the identified metabolite features using the KEGG metabolic pathway database. The compounds identified in the uninfected and SLCMV–infected cassava plants are denoted.

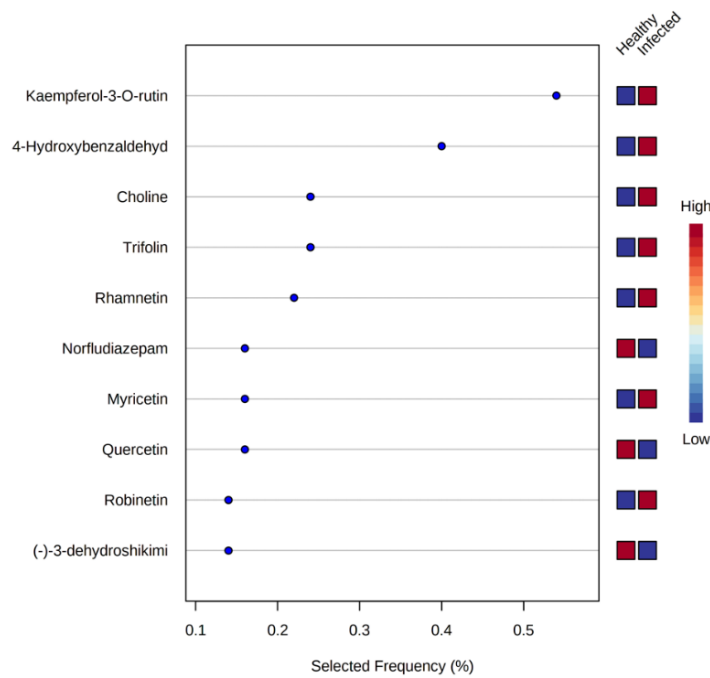


**Figure 9.** Graphical representation of the most important metabolite features for biomarker analysis. The performance of the biomarker models created using the automated import feature identification function in the MetaboAnalystR database was evaluated by ROC curve analysis. The 10 identified features were identified as biomarkers for the prediction of healthy and infected cassava plants. The blue and red bars refer to healthy and SLCMV-infected cassava plants, respectively.

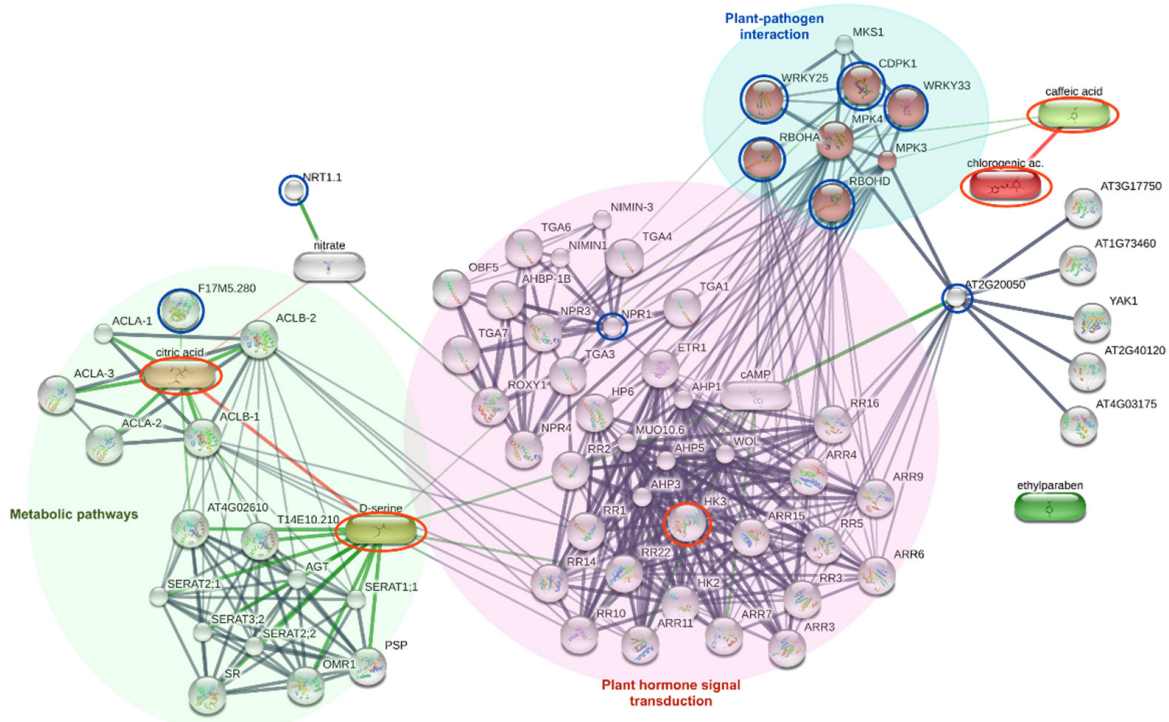


**Figure 10.** The interactions of the nine proteins and five metabolites identified by proteomics and metabolomics profiling of the SLCMV-infected cassava plants were determined with STITCH. The red and blue circles denote the identified metabolites and proteins, respectively.

#### 4. Discussion

Proteomics analyses are performed for the identification and analysis of proteins. This approach aids in understanding the functions of genes and enables the comprehensive analysis of proteins, which is useful in crop improvement strategies [23]. Previous studies have successfully employed proteomics tools for elucidating the mechanisms underlying plant resistance, including the analysis of spatial proteomes and post-translational modifications (PTMs) of proteins, which are directly involved in the plant immune response [24]. Proteomics, in contrast, can aid in identifying key metabolic processes and determining the potential interactions with crucial regulatory pathways. Metabolomics analysis is used for detecting the metabolite end products of different regulatory processes and can effectively elucidate the molecular mechanisms underlying any variations in plants at the transcriptional and translational levels [25].

Numerous studies have identified the mechanisms underlying the alterations in the composition of proteins and metabolites in plants during the biotic stress response, and the present study aimed to understand the regulatory mechanism of the major plant responses [26–31]. As plant–pathogen interactions are spatially dynamic processes, the bioactive effects of secondary metabolites on plant immunity depend on their accumulation at an optimum concentration at a specific time in specific plant intracellular regions [32]. The integration of proteomics and metabolomics analyses is a novel strategy for deciphering the mechanisms underlying the resistance to pathogen-induced stress in plants and primarily allows the quantitative analysis and identification of candidate genes that can be employed in breeding programs.

The integrated proteomics and metabolomics approach used in this study enabled us to identify whether the pattern in which the proteins and metabolites were arranged in the networks had a strong relationship with the three enriched KEGG pathways, namely, the plant–pathogen interaction pathway, plant hormone signal transduction pathway, and metabolic pathways. Integrated proteomics and metabolomics analysis is emerging as a cutting-edge approach in functional biology for understanding plant responses to biotic stresses at cellular and developmental stages. The integration of the results of these approaches with genomics data allows the accurate identification of candidate genes and pathways related to important agronomical traits, including disease-resistant phenotypes, that can be applied to crop breeding programs [33].

The compatibility of plant–pathogen interactions usually involves temporal oxidative bursts for pathogen detection and signaling that lead to hypersensitive response (HR) and programmed cell death (PDC), which create a delimited zone that prevents the growth and spread of the pathogen [34]. The findings of this study indicated that these proteins and metabolites, including RBOHA, RBOHD, WRKY25, caffeic acid, and CGA, play important key roles in the generation of ROS. The defense mechanisms that are triggered during plant–virus interactions primarily induce the accumulation of ROS. Notably, ROS play a dual role in pathogen restriction and are frequently localized in apoptotic cells at the sites of infection; they also induce antioxidant and pathogenesis-related defense responses in the neighboring plant cells by acting as a diffusible signal [35–38]. Plant respiratory burst oxidase homologs (RBOGS) are also referred to as nicotinamide adenine dinucleotide phosphate (NADPH) oxidases (NOXs). NOXs can integrate different signal transduction pathways; for instance, they can integrate calcium signaling pathways, protein phosphorylation cascades catalyzed by protein kinases, nitric oxide pathways, and pathways mediated by lipid messengers [39]. Doll et al. demonstrated that WRKY25 partakes in regulating intracellular redox conditions, and the overexpression of WRKY25 increases the tolerance to oxidative stress [40]. Normally, WRKY TFs are key regulatory components of defense-related genes.

A recent study demonstrated that MAP kinase 4 (MPK4) of *Arabidopsis* sp. interacts with an MPK4 substrate (MKS1), which in turn interacts with WRKY25 and WRKY33 [41]. In vitro experiments have demonstrated that WRKY25 and WRKY33 are substrates of MPK4. These findings indicated that WRKY25 and WRKY33 function as downstream components of the MPK4-mediated signaling pathway and contribute to the suppression

of SA-dependent disease resistance. Additionally, a study by Zheng et al. suggested that WRKY33 is an important component of the regulatory cascade and mediates cross-talk between the defense responses to pathogens and the different mechanisms of pathogenesis that are induced in response to *Pseudomonas syringae* infections [42]. WRKY 33 is translocated to the nucleus of plant cells, where it recognizes and binds to the TTGACC sequence of W-box to induce the expression of genes involved in plant defense or defense-related genes, including PR genes and NPR1 [43]. Furthermore, WRKY33 can act as a positive regulator of the defense response signaling pathways mediated by JA and ET [42]. Interestingly, the results of proteomics and STITCH analyses demonstrated that CDPK1 was integrated with RBOGS via WRKY25 and WRKY33 (Figures 5 and 10). The expression levels of both the proteins in healthy and SLCMV-infected plants were high and low, respectively. The mechanism of defense of the SLCMV-infected KU 50 variety of cassava can be explained by comparing the results of previous studies with our findings, especially in terms of ROS accumulation and the differential expression of WRKY25 and WRKY33. The KU50 variety is tolerant to SLCMV and was the platform in this study. This variety can also be used to investigate how different cultivars with variable resistance and susceptibility respond to SLCMV.

Among the proteins and metabolites that were expressed at high levels in the cassava plants with CMD, we found that caffeic acid and CGA interacted with the proteins that act cooperatively during the production of ROS and in the processes of plant defense. CGA is an important phenolic compound that belongs to the hydroxycinnamic acid family and produces caffeic acid and quinic acid following esterification [44].

CGA and its derivatives comprise a group of secondary metabolites that are associated with the transcriptional activation of phenylpropanoid pathways under pathogen infection and conditions of biotic stress [45]. CGA and CGA-derived metabolites play indispensable roles in plant defense and redox reactions [46]. Numerous studies have demonstrated that CGA participates in plant defense reactions. For instance, a study by Jiang et al. [47] demonstrated that the expression of *PbSPMS*, which mediates spermine synthesis, contributes to the biosynthesis of CGA in *Arabidopsis* sp. and improves plant resistance to drought and salt stress. Another study by Atanasova-Penichon, et al. [48] demonstrated that CGA plays a role in the defense response of maize against *Fusarium graminearum* and the accumulation of trichothecene. The study also reported that more resistant varieties have higher levels of CGA [49]. Wojciechowska et al. demonstrated that CGA reduces the colonization of *Alternaria alternata* in tomato fruits by inhibiting toxin synthesis [50]. The putative role of CGA in defense was determined by metabolomic analysis of variably resistant varieties. The findings revealed that the accumulation of CGA was higher in the resistant variety that suppressed *A. alternata* infections. Based on the results of previous studies and the findings obtained herein, the present study indicated that CGA might play an important role in the mechanism of plant defense, especially in terms of ROS accumulation in the SLCMV-tolerant KU50 variety of cassava. However, the regulatory mechanisms of CGA biosynthesis, including the responses of the genetic regulatory networks of CGA biosynthesis, remain to be elucidated in different SLCMV-infected varieties of cassava.

The results of STITCH analysis of the protein–metabolite interactions revealed that caffeic acid integrated CGA and the proteins associated with plant–pathogen interactions. These findings supported the fact that caffeic acid and CGA are involved in the mechanism of plant defense. Caffeic acid is involved in plant biotic and abiotic stress tolerance, including pathogen attacks, low and high-temperature stress, UV light, drought, heavy metal stress, and salinity stress [51]. In a study by Juan [52], plants were exposed to invading pathogens during the increased accumulation of caffeic acid, and the findings revealed that high levels of caffeic acid during fungal infections prevent the formation of brown rot. The increased accumulation of caffeic acid improves disease resistance in apples by reducing the activity of the pathogens. Other studies have also demonstrated that the exogenous application of caffeic acid significantly improves disease resistance in plants [53]. Additionally, Davidson et al. [54] reported that the growth of several *Fusarium*

spp. and *Saccharomyces* spp. is inhibited by the application of 500 µg/mL caffeine. However, further studies are necessary to determine the potential uses of CGA, caffeic acid, and their derivatives in the treatment of SLCMV.

The results of integrated proteomics and metabolomics analysis revealed that the identified proteins and metabolites acted as intermediaries in integrating the functions of the different components. The present study revealed that the plant–pathogen interaction pathway was linked to plant hormone signal transduction, while the metabolic pathways were associated with hormone signal transduction. Numerous studies have demonstrated that the interactions between plants and pathogens also upregulate primary metabolism in plants. Rojas et al. [55] suggested that an increase in primary metabolism alters the signaling processes that trigger plant defense reactions. Similar to a study by Kangasjärvi et al. [55], Bolton [56] suggested that primary metabolism provides the cellular energy required for plant defense responses during plant–pathogen interactions. The finding is also consistent with a review by Rojas et al. [57], which reported that the expression of several genes associated with primary metabolic pathways, including those involved in the synthesis or degradation of carbohydrates, amino acids, and lipids, are induced in plants following exposure to pathogens or elicitors. However, further studies are necessary to fully understand the complexity of the plant defense response in cassava plants infected with SLCMV.

Altogether, the present study revealed that the levels of five important metabolites were significantly altered in cassava plants following infection with SLCMV (Figure 9). The putative targets were also identified in this study for future breeding efforts. The majority of metabolites were chemically classified as flavonoids or their derivatives. A previous study has demonstrated that flavonoids and other phenolic compounds play important roles in plant immunity [58]. We propose that the five metabolites identified herein could serve as potential biomarkers for the identification of SLCMV-infected cassava plants and are described in detail hereafter.

Kaempferol-3-O-rutin was identified as one of the potential biomarkers of SLCMV infection in this study. Kaempferol-3-O-rutin is a flavonoid and a major secondary metabolite derived from the phenylpropanoid pathway in plants [59]. An et al. [60] reported that kaempferol induces disease resistance by activating NPR1 in an MPK- and SA-dependent manner. Another study by An et al. [61] provided further evidence regarding the application of kaempferol in plant disease resistance. The results confirmed that kaempferol effectively induces plant defense against *P. syringae* pv. *tomato* DC3000 (*Pst* DC3000). SLCMV may activate the phenylpropanoid pathway of cassava to stimulate the production of kaempferol during infection. However, the mechanism of action of kaempferol in cassava plants with SLCMV infection remains to be determined.

The secondary metabolite, 4-hydroxybenzaldehyde, possesses anti-diabetic, antioxidant, and pro-angiogenic properties [62–64], and a recent study by Kim et al. [65] demonstrated that 4-hydroxybenzaldehyde regulates immune tolerance and aggravated inflammatory responses in humans. A previous study identified and characterized 4-hydroxybenzaldehyde during grapevine trunk disease caused by *Diaporthe eres*, and the results demonstrated that 4-hydroxybenzaldehyde was one of the phytotoxic metabolites that were detected following infection [66]. Yu et al. [67] used 4-hydroxybenzaldehyde as an intermediate during the synthesis of (*E*)-4-(4-hydroxyphenyl) but-3-en-2-one to prepare a series of 1,4-pentadien-3-one derivatives containing a 1,3,4-thiadiazole moiety, for determining their curative, protective, and inactivating potential against *Tobacco mosaic virus* (TMV). The results demonstrated that the compounds had excellent anti-TMV activity, which can be employed for the development of novel antiviral agents. In the present study, 4-hydroxybenzaldehyde was detected in cassava plants infected with SLCMV. The study indicated that 4-hydroxybenzaldehyde could be one of the potent compounds produced by cassava plants against SLCMV infection, and the findings are consistent with the results of previous studies. Nevertheless, there is a scarcity of information regarding the potential of

4-hydroxybenzaldehyde in combating plant viruses, and further studies are necessary in this regard.

Choline is one of the main components of eukaryotic membrane lipids, and choline can be detected in cells only after the appearance of phosphatidylcholine (PC) [68]. Choline is produced during the degradation of PC, and it changes into the active form, phospholipase D (PLD) [69,70]. Choline is normally produced by soybean [71], and Chen et al. [72] reported that *P. syringae*, a common pathogenic bacterium associated with various plant species, has adapted to exploit and utilize the choline produced for the physiological activities of soybean plants. The results of the present study demonstrated that high levels of choline had accumulated in cassava plants infected with SLCMV. The association between choline and plant viruses has not been previously reported; therefore, this finding has significant implications for future studies on plant viruses, the metabolic processes involved in plant defense mechanisms, and viral progression.

Trifolin is a flavonoid that is commonly detected in a wide range of plants and possesses bactericidal and antifungal properties [73,74]. However, Funayama et al. [75] reported that trifolin is inactive against yeasts. Unfortunately, the antiviral properties of trifolin in plants have not been elucidated to date. The antiviral potential of trifolin has been extensively studied against the human virus, SARS-CoV-2. Recently, Makati et al. [76] investigated the interactions of the flavonoids, afzelin and trifolin with the 3CLpro, Nsp1, Nsp3, RdRp, Nsp7-Nsp8 complex, and PLpro proteins of SARS-CoV-2 using molecular docking approaches. The results demonstrated that the RdRp, Nsp7-Nsp8 complex, and Nsp3 protein of SARS-CoV-2, which are related to viral replication, virulence, and viral spread, formed the highest number of interactions with trifolin. The proteins encoded by the SLCMV genome could be similarly docked to trifolin to elucidate the mechanism underlying the antiviral effect of trifolin in cassava plants.

Rhamnetin is a phenolic flavonoid and a methylated derivative of quercetin. Rhamnetin possesses the anti-inflammatory potential and inhibits the enzymatic activity of secretory phospholipase A2, which plays an important role during acute inflammation [77]. Nawrot et al. [78] suggested that rhamnetin could be a candidate natural compound for the development of novel anti-inflammatory drugs. However, compared to the number of studies on humans, few studies have investigated the effects of rhamnetin against plant diseases.

The five aforementioned metabolites have also been thoroughly investigated in human diseases, especially against SARS-CoV-2. The approaches used for studying their effects against human diseases can also be employed in plants to determine their antiviral potential against plant diseases. Altogether, this study identified that the levels of five metabolites, namely, kaempferol-3-O-rutin, 4-hydroxybenzaldehyde, choline, trifolin, and rhamnetin, were increased in cassava plants infected with SLCMV, compared with healthy plants. However, the association between these five compounds and the defense system of plants during viral infections remains to be elucidated.

## 5. Conclusions

Proteomics and metabolomics analysis of the SLCMV-infected and healthy cassava cv. Kasetart 50 revealed changes in the regulation of protein abundance and metabolites. Proteomics analyses discovered that 359 proteins were particularly enriched in the plant-pathogen interaction, plant hormone signal transduction, and MAPK signaling pathways. By analyzing the metabolomes of the healthy and SLCMV-infected cassava plants, a total of 79 substances were revealed. In 11 KEGG pathways, 9 proteins and 5 metabolites were found to be enriched, according to integrated omics analysis, specifically the plant hormone signal transduction and plant-pathogen interaction pathways.

Moreover, KEGG functional enrichment analysis revealed that plant-pathogen interaction, plant hormone signal transduction, and metabolic pathways were linked via the enriched protein (protein phosphatase 2C) and metabolites (cyclic nucleotide-binding (AT2G20050) and D-serine). The result indicated that proteomics and metabolomics analy-

sis could describe the pathogen and host interaction mechanisms and aid in cassava crop improvement programs. The findings would also help in developing the cassava plant's defense response network and in identifying the potential proteins and metabolites for selecting a particular SLCMV-resistant variety.

**Author Contributions:** The authors confirm their contribution to the paper as follows: study conception and design: W.S., S.R. and S.M.; data collection: N.V. and S.C. (Somruthai Chaowongdee). Author; analysis and interpretation of results: W.S., S.R., S.C. (Sawanya Charoenlappanit), P.P., A.P., N.V., S.C. (Somruthai Chaowongdee) and S.M.; draft manuscript preparation: W.S. and S.M. All authors have read and agreed to the published version of the manuscript.

**Funding:** This research was supported by Kasetsart University Research and Development (KURDI), FF(KU)18.65.

**Data Availability Statement:** The datasets generated and analyzed in the current study are available in ProteomeXchange; accession number PXD035792 and the ScienceDB database <https://www.scidb.cn/en/s/uAbEzq> accessed on 12 January 2023 for proteomics and metabolomics analysis, respectively.

**Acknowledgments:** We thank the Thai Tapioca Development Institute (TTDI) for support with the cassava planting materials.

**Conflicts of Interest:** The authors declare no conflict of interest.

## References

1. Wang, H.L.; Cui, X.Y.; Wang, X.W.; Liu, S.S.; Zhang, Z.H.; Zhou, X.P. First report of Sri Lankan cassava mosaic virus infecting cassava in Cambodia. *Plant Dis.* **2016**, *100*, 1029. [[CrossRef](#)]
2. Uke, A.; Hoat, T.X.; Quan, M.V.; Liem, N.V.; Ugaki, M.; Natsuaki, K.T. First report of Sri Lankan cassava mosaic virus infecting cassava in Vietnam. *Plant Dis.* **2018**, *102*, 2669. [[CrossRef](#)]
3. Siriwan, W.; Jimenez, J.; Hemniam, N.; Saokham, K.; Lopez-Alvarez, D.; Leiva, A.M.; Martinez, A.; Mwanzia, L.; Becerra Lopez-Lavalle, L.A.; Cuellar, W.J. Surveillance and diagnostics of the emergent Sri Lankan cassava mosaic virus (Fam. Geminiviridae) in Southeast Asia. *Virus Res.* **2020**, *285*, 197959. [[CrossRef](#)]
4. Chittarath, K.; Jimenez, J.; Vongphachanh, P.; Leiva, A.M.; Sengsay, S.; Lopez-Alvarez, D.; Bounvilayvong, T.; Lourido, D.; Vorlachith, V.; Cuellar, W.J. First report of cassava mosaic disease and Sri Lankan cassava mosaic virus in Laos. *Plant Dis.* **2021**, *105*, 1861. [[CrossRef](#)] [[PubMed](#)]
5. Malik, A.I.; Sophearith, S.; Delaquis, E.; Cuellar, W.J.; Jimenez, J.; Newby, J.C. Susceptibility of cassava varieties to disease caused by Sri Lankan cassava mosaic virus and impacts on yield by use of asymptomatic and virus-free planting material. *Agronomy* **2022**, *12*, 1658. [[CrossRef](#)]
6. Gracen, V.E.; Kongsil, P.; Napasintuwong, O.; Duangjit, J.; Phumichai, C. *The Story of Kasetsart 50: The Most Important Cassava Variety in the World*; Center of Agricultural Biotechnology, Kasetsart University: Bangkok, Thailand, 2018; p. 53.
7. Hemniam, N.; Saokham, K.; Roekwan, S.; Hunsawattanakul, S.; Thawinampan, J.; Siriwan, W. Severity of cassava mosaic disease in resistance and commercial varieties by grafting. In Proceedings of the 14th National Plant Protection Conference, Phetchaburi, Thailand, 12–14 November 2019; Volume 794, p. 799.
8. Delaquis, E.; Andersen, K.F.; Minato, N.; Cu, T.T.L.; Karssenberg, M.E.; Sok, S.; Wyckhuys, K.A.G.; Newby, J.C.; Burra, D.D.; Srean, P.; et al. Raising the stakes: Cassava seed networks at multiple scales in Cambodia and Vietnam. *Front. Sustain. Food Syst.* **2018**, *2*, 1–21. [[CrossRef](#)]
9. Saokham, K.; Hemniam, N.; Roekwan, S.; Hunsawattanakul, S.; Thawinampan, J.; Siriwan, W. Survey and molecular detection of Sri Lankan cassava mosaic virus in Thailand. *PLoS ONE* **2021**, *16*, e0252846. [[CrossRef](#)] [[PubMed](#)]
10. Götz, M.; Winter, S. Diversity of *Bemisia tabaci* in Thailand and Vietnam and indications of species replacement. *J. Asia-Pac. Entomol.* **2016**, *19*, 537–543. [[CrossRef](#)]
11. Bigeard, J.; Colcombet, J.; Hirt, H. Signaling mechanisms in pattern-triggered immunity (PTI). *Mol. Plant* **2015**, *8*, 521–539. [[CrossRef](#)]
12. Jones, J.D.; Dangl, J.L. The plant immune system. *Nature* **2006**, *444*, 323–329. [[CrossRef](#)] [[PubMed](#)]
13. Jain, P.; Dubey, H.; Singh, P.K.; Solanke, A.U.; Singh, A.K.; Sharma, T.R. Deciphering signalling network in broad spectrum Near Isogenic Lines of rice resistant to *Magnaporthe oryzae*. *Sci. Rep.* **2019**, *9*, 16939. [[CrossRef](#)] [[PubMed](#)]
14. Wu, X.; Gong, F.; Cao, D.; Hu, X.; Wang, W. Advances in crop proteomics: PTMs of proteins under abiotic stress. *Proteomics* **2016**, *16*, 847–865. [[CrossRef](#)] [[PubMed](#)]
15. Erb, M.; Kliebenstein, D.J. Plant secondary metabolites as defenses, regulators, and primary metabolites: The blurred functional trichotomy. *Plant Physiol.* **2020**, *184*, 39–52. [[CrossRef](#)] [[PubMed](#)]
16. Doyle, J.J. A rapid DNA isolation procedure for small quantities of fresh leaf tissue. *Phytochem. Bull.* **1987**, *19*, 11–15.

17. Lowry, O.H.; Rosebrough, N.J.; Farr, A.L.; Randall, R.J. Protein measurement with the Folin phenol reagent. *J. Biol. Chem.* **1951**, *193*, 265–275. [[CrossRef](#)]
18. Tyanova, S.; Temu, T.; Sinitcyn, P.; Carlson, A.; Hein, M.Y.; Geiger, T.; Mann, M.; Cox, J. The Perseus computational platform for comprehensive analysis of (prote)omics data. *Nat. Methods* **2016**, *13*, 731–740. [[CrossRef](#)]
19. Howe, E.A.; Sinha, R.; Schlauch, D.; Quackenbush, J. RNA-Seq analysis in MeV. *Bioinformatics* **2011**, *27*, 3209–3210. [[CrossRef](#)]
20. Mi, H.; Muruganujan, A.; Ebert, D.; Huang, X.; Thomas, P.D. PANTHER version 14: More genomes, a new PANTHER GO-slim and improvements in enrichment analysis tools. *Nucleic Acids Res.* **2019**, *47*, D419–D426. [[CrossRef](#)]
21. Chong, J.; Soufan, O.; Li, C.; Caraus, I.; Li, S.; Bourque, G.; Wishart, D.S.; Xia, J. MetaboAnalyst 4.0: Towards more transparent and integrative metabolomics analysis. *Nucleic Acids Res.* **2018**, *46*, W486–W494. [[CrossRef](#)]
22. Kanehisa, M.; Goto, S. KEGG: Kyoto encyclopedia of genes and genomes. *Nucleic Acids Res.* **2000**, *28*, 27–30. [[CrossRef](#)]
23. Tan, B.C.; Lim, Y.S.; Lau, S.E. Proteomics in commercial crops: An overview. *J. Proteom.* **2017**, *169*, 176–188. [[CrossRef](#)]
24. Liu, Y.; Lu, S.; Liu, K.; Wang, S.; Huang, L.; Guo, L. Proteomics: A powerful tool to study plant responses to biotic stress. *Plant Methods* **2019**, *15*, 135. [[CrossRef](#)] [[PubMed](#)]
25. Arbona, V.; Manzi, M.; Ollas, C.D.; Gómez-Cadenas, A. Metabolomics as a tool to investigate abiotic stress tolerance in plants. *Int. J. Mol. Sci.* **2013**, *14*, 4885–4911. [[CrossRef](#)] [[PubMed](#)]
26. Chen, F.; Ma, R.; Chen, X.-L. Advances of metabolomics in fungal pathogen–plant interactions. *Metabolites* **2019**, *9*, 169. [[CrossRef](#)]
27. Kushalappa, A.C.; Gunnaiah, R. Metabolo-proteomics to discover plant biotic stress resistance genes. *Trends Plant Sci.* **2013**, *18*, 522–531. [[CrossRef](#)]
28. Sarwat, M.; Ahmad, A.; Abidin, M.; Ibrahim, M.M. *Stress Signaling in Plants: Genomics and Proteomics Perspective*, 1st ed.; Springer: New York, NY, USA, 2013; Volume 2, p. XI-233.
29. Feussner, I.; Polle, A. What the transcriptome does not tell—Proteomics and metabolomics are closer to the plants' pathophenotype. *Curr. Opin. Plant Biol.* **2015**, *26*, 26–31. [[CrossRef](#)] [[PubMed](#)]
30. Alexander, M.M.; Cilia, M. A molecular tug-of-war: Global plant proteome changes during viral infection. *Curr. Plant Biol.* **2016**, *5*, 13–24. [[CrossRef](#)]
31. Peyraud, R.; Dubiella, U.; Barbacci, A.; Genin, S.; Raffaele, S.; Roby, D. Advances on plant–pathogen interactions from molecular toward systems biology perspectives. *Plant J.* **2017**, *90*, 720–737. [[CrossRef](#)] [[PubMed](#)]
32. Piasecka, A.; Jedrzejczak-Rey, N.; Bednarek, P. Secondary metabolites in plant innate immunity: Conserved function of divergent chemicals. *New Phytol.* **2015**, *206*, 948–964. [[CrossRef](#)]
33. Langridge, P.; Fleury, D. Making the most of 'omics' for crop breeding. *Trends Biotechnol.* **2011**, *29*, 33–40. [[CrossRef](#)] [[PubMed](#)]
34. Barna, B.; Fodor, J.; Harrach, B.; Pogány, M.; Király, Z. The Janus face of reactive oxygen species in resistance and susceptibility of plants to necrotrophic and biotrophic pathogens. *Plant Physiol. Biochem.* **2012**, *59*, 37–43. [[CrossRef](#)] [[PubMed](#)]
35. Hernández, J.A.; Gullner, G.; Clemente-Moreno, M.J.; Künstler, A.; Juhász, C.; Díaz-Vivancos, P.; Király, L. Oxidative stress and antioxidative responses in plant–virus interactions. *Physiol. Mol. Plant Pathol.* **2016**, *94*, 134–148. [[CrossRef](#)]
36. Bacsó, R.; Hafez, Y.; Király, Z.; Király, L. Inhibition of virus replication and symptom expression by reactive oxygen species in tobacco infected with Tobacco mosaic virus. *Acta Phytopathol. Entomol. Hung.* **2011**, *46*, 1–10. [[CrossRef](#)]
37. Díaz-Vivancos, P.; Clemente-Moreno, M.J.; Rubio, M.; Olmos, E.; García, J.A.; Martínez-Gómez, P.; Hernández, J.A. Alteration in the chloroplastic metabolism leads to ROS accumulation in pea plants in response to plum pox virus. *J. Exp. Bot.* **2008**, *59*, 2147–2160. [[CrossRef](#)]
38. Hafez, Y.M.; Bacsó, R.; Király, Z.; Künstler, A.; Király, L. Up-regulation of antioxidants in tobacco by low concentrations of H<sub>2</sub>O<sub>2</sub> suppresses necrotic disease symptoms. *Phytopathology* **2012**, *102*, 848–856. [[CrossRef](#)]
39. Wang, W.; Chen, D.; Zhang, X.; Liu, D.; Cheng, Y.; Shen, F. Role of plant respiratory burst oxidase homologs in stress responses. *Free Radical Res.* **2018**, *52*, 826–839. [[CrossRef](#)]
40. Doll, J.; Muth, M.; Riester, L.; Nebel, S.; Bresson, J.; Lee, H.-C.; Zentgraf, U. *Arabidopsis thaliana* WRKY25 transcription factor mediates oxidative stress tolerance and regulates senescence in a redox-dependent manner. *Front. Plant Sci.* **2020**, 1–19. [[CrossRef](#)]
41. Andreasson, E.; Jenkins, T.; Brodersen, P.; Thorgrimsen, S.; Petersen, N.H.; Zhu, S.; Qiu, J.L.; Micheelsen, P.; Rocher, A.; Petersen, M. The MAP kinase substrate MKS1 is a regulator of plant defense responses. *EMBO J.* **2005**, *24*, 2579–2589. [[CrossRef](#)]
42. Zheng, Z.; Qamar, S.A.; Chen, Z.; Mengiste, T. *Arabidopsis* WRKY33 transcription factor is required for resistance to necrotrophic fungal pathogens. *Plant J.* **2006**, *48*, 592–605. [[CrossRef](#)]
43. Yu, D.; Chen, C.; Chen, Z. Evidence for an important role of WRKY DNA binding proteins in the regulation of NPR1 gene expression. *Plant Cell* **2001**, *13*, 1527–1540. [[CrossRef](#)]
44. Santana-Gálvez, J.; Cisneros-Zevallos, L.; Jacobo-Velázquez, D.A. Chlorogenic acid: Recent advances on its dual role as a food additive and a nutraceutical against metabolic syndrome. *Molecules* **2017**, *22*, 358. [[CrossRef](#)] [[PubMed](#)]
45. Osmond, C.B.; Foyer, C.H.; Bock, G.; Grace, S.C.; Logan, B.A. Energy dissipation and radical scavenging by the plant phenylpropanoid pathway. *Philos. Trans. R. Soc. Lond. Ser. B Biol. Sci.* **2000**, *355*, 1499–1510. [[CrossRef](#)]
46. Pandey, A.; Misra, P.; Bhambhani, S.; Bhatia, C.; Trivedi, P.K. Expression of *Arabidopsis* MYB transcription factor, AtMYB111, in tobacco requires light to modulate flavonol content. *Sci. Rep.* **2014**, *4*, 5018. [[CrossRef](#)] [[PubMed](#)]
47. Jiang, X.; Zhan, J.; Wang, Q.; Wu, X.; Chen, X.; Jia, B.; Liu, P.; Liu, L.; Ye, Z.; Zhu, L.; et al. Overexpression of the pear *PbSPMS* gene in *Arabidopsis thaliana* increases resistance to abiotic stress. *Plant Cell Tissue Organ Cult.* **2020**, *140*, 389–401. [[CrossRef](#)]

48. Atanasova-Penichon, V.; Pons, S.; Pinson-Gadais, L.; Picot, A.; Marchegay, G.; Bonnin-Verdal, M.-N.; Ducos, C.; Barreau, C.; Roucolle, J.; Sehabiague, P. Chlorogenic acid and maize ear rot resistance: A dynamic study investigating *Fusarium graminearum* development, deoxynivalenol production, and phenolic acid accumulation. *Mol. Plant-Microbe Interact.* **2012**, *25*, 1605–1616. [[CrossRef](#)] [[PubMed](#)]
49. Wang, L.-J.; Li, J.-H.; Gao, J.-J.; Feng, X.-X.; Shi, Z.-X.; Gao, F.-Y.; Xu, X.-L.; Yang, L.-Y. Inhibitory effect of chlorogenic acid on fruit russetting in ‘Golden Delicious’ apple. *Sci. Hort.* **2014**, *178*, 14–22. [[CrossRef](#)]
50. Wojciechowska, E.; Weinert, C.H.; Egert, B.; Trierweiler, B.; Schmidt-Heydt, M.; Horneburg, B.; Graeff-Hönninger, S.; Kulling, S.E.; Geisen, R. Chlorogenic acid, a metabolite identified by untargeted metabolome analysis in resistant tomatoes, inhibits the colonization by *Alternaria alternata* by inhibiting alternariol biosynthesis. *Eur. J. Plant Pathol.* **2014**, *139*, 735–747. [[CrossRef](#)]
51. Douglas, C.J. Phenylpropanoid metabolism and lignin biosynthesis: From weeds to trees. *Trends Plant Sci.* **1996**, *1*, 171–178. [[CrossRef](#)]
52. Juan, A.M. Natural fungicides obtained from plants. In *Fungicides for Plant and Animal Diseases*; Dhanasekaran, D., Thajuddin, N., Panneerselvam, A., Eds.; IntechOpen: Rijeka, Croatia, 2012; p. 310.
53. Barkai-Golan, R. *Postharvest Diseases of Fruits and Vegetables: Development and Control*; Elsevier: Amsterdam, The Netherlands, 2018; pp. 1–52.
54. Davidson, P.M.; Taylor, T.M.; Schmidt, S.E. Chemical preservatives and natural antimicrobial compounds. In *Food Microbiology: Fundamentals and Frontiers*, 4th ed.; Wiley Online Library: Hoboken, NJ, USA, 2012; pp. 765–801. [[CrossRef](#)]
55. Kangasjärvi, S.; Neukermans, J.; Li, S.; Aro, E.-M.; Noctor, G. Photosynthesis, photorespiration, and light signalling in defence responses. *J. Exp. Bot.* **2012**, *63*, 1619–1636. [[CrossRef](#)]
56. Bolton, M.D. Primary metabolism and plant defense—Fuel for the fire. *Mol. Plant-Microbe Interact.* **2009**, *22*, 487–497. [[CrossRef](#)]
57. Rojas, C.; Senthil-Kumar, M.; Tzin, V.; Mysore, K. Regulation of primary plant metabolism during plant–pathogen interactions and its contribution to plant defense. *Front. Plant Sci.* **2014**, *5*, 17. [[CrossRef](#)] [[PubMed](#)]
58. Iranshahi, M.; Rezaee, R.; Parhiz, H.; Roohbakhsh, A.; Soltani, F. Protective effects of flavonoids against microbes and toxins: The cases of hesperidin and hesperetin. *Life Sci.* **2015**, *137*, 125–132. [[CrossRef](#)] [[PubMed](#)]
59. Falcone Ferreyra, M.L.; Rius, S.P.; Casati, P. Flavonoids: Biosynthesis, biological functions, and biotechnological applications. *Front. Plant Sci.* **2012**, *3*, 222. [[CrossRef](#)] [[PubMed](#)]
60. An, J.; Kim, S.H.; Bahk, S.; Vuong, U.T.; Nguyen, N.T.; Do, H.L.; Kim, S.H.; Chung, W.S. Naringenin induces pathogen resistance against *Pseudomonas syringae* through the activation of NPR1 in *Arabidopsis*. *Front. Plant Sci.* **2021**, *12*, 853. [[CrossRef](#)] [[PubMed](#)]
61. An, J.; Nguyen, X.C.; Kim, S.H.; Bahk, S.; Kang, H.; Le Anh Pham, M.; Park, J.; Ramadany, Z.; Kim, S.H.; Park, H.C.; et al. Kaempferol promotes bacterial pathogen resistance through the activation of NPR1 by both SA and MPK signaling pathways in *Arabidopsis*. *Plant Biotechnol. Rep.* **2022**, *16*, 655–663. [[CrossRef](#)]
62. Park, S.; Kim, D.S.; Kang, S. *Gastrodia elata* blume water extracts improve insulin resistance by decreasing body fat in diet-induced obese rats: Vanillin and 4-hydroxybenzaldehyde are the bioactive candidates. *Eur. J. Nutr.* **2011**, *50*, 107–118. [[CrossRef](#)]
63. Ha, J.-H.; Lee, D.-U.; Lee, J.-T.; Kim, J.-S.; Yong, C.-S.; Kim, J.-A.; Ha, J.-S. 4-Hydroxybenzaldehyde from *Gastrodia elata* B1. is active in the antioxidation and GABAergic neuromodulation of the rat brain. *J. Ethnopharmacol.* **2000**, *73*, 329–333. [[CrossRef](#)]
64. Kang, C.; Han, Y.; Kim, J.; Oh, J.; Cho, Y.; Lee, E. 4-Hydroxybenzaldehyde accelerates acute wound healing through activation of focal adhesion signalling in keratinocytes. *Sci. Rep.* **2017**, *7*, 14192. [[CrossRef](#)]
65. Kim, W.S.; Song, H.-Y.; Mushtaq, S.; Kim, J.-M.; Byun, E.-H.; Yuk, J.-M.; Byun, E.-B. Therapeutic potential of gamma-irradiated resveratrol in ulcerative colitis via the anti-inflammatory activity and differentiation of tolerogenic dendritic cells. *Cell Physiol. Biochem.* **2019**, *52*, 1117–1138.
66. Reveglia, P.; Pacetti, A.; Masi, M.; Cimmino, A.; Carella, G.; Marchi, G.; Mugnai, L.; Evidente, A. Phytotoxic metabolites produced by *Diaporthe eres* involved in cane blight of grapevine in Italy. *Nat. Prod. Res.* **2021**, *35*, 2872–2880. [[CrossRef](#)]
67. Yu, L.; Gan, X.; Zhou, D.; He, F.; Zeng, S.; Hu, D. Synthesis and antiviral activity of novel 1,4-pentadien-3-one derivatives containing a 1,3,4-thiadiazole moiety. *Molecules* **2017**, *22*, 658. [[CrossRef](#)] [[PubMed](#)]
68. Datko, A.H.; Mudd, S.H. Phosphatidylcholine synthesis: Differing patterns in soybean and carrot. *Plant Physiol.* **1988**, *88*, 854–861. [[CrossRef](#)] [[PubMed](#)]
69. Welti, R.; Li, W.; Li, M.; Sang, Y.; Biesiada, H.; Zhou, H.-E.; Rajashekar, C.; Williams, T.D.; Wang, X. Profiling membrane lipids in plant stress responses: Role of phospholipase D $\alpha$  in freezing-induced lipid changes in *Arabidopsis*. *J. Biol. Chem.* **2002**, *277*, 31994–32002. [[CrossRef](#)] [[PubMed](#)]
70. Bargmann, B.O.; Laxalt, A.M.; Riet, B.T.; Testerink, C.; Merquiol, E.; Mosblech, A.; LEON-REYES, A.; Pieterse, C.M.; Haring, M.A.; Heilmann, I. Reassessing the role of phospholipase D in the *Arabidopsis* wounding response. *Plant Cell Environ.* **2009**, *32*, 837–850. [[CrossRef](#)]
71. Keogh, M.R.; Courtney, P.D.; Kinney, A.J.; Dewey, R.E. Functional characterization of phospholipid N-methyltransferases from *Arabidopsis* and soybean. *J. Biol. Chem.* **2009**, *284*, 15439–15447. [[CrossRef](#)]
72. Chen, C.; Li, S.; McKeever, D.R.; Beattie, G.A. The widespread plant-colonizing bacterial species *Pseudomonas syringae* detects and exploits an extracellular pool of choline in hosts. *Plant J.* **2013**, *75*, 891–902. [[CrossRef](#)]
73. Van der Watt, E.; Pretorius, J.C. Purification and identification of active antibacterial components in *Carpobrotus edulis* L. *J. Ethnopharmacol.* **2001**, *76*, 87–91. [[CrossRef](#)]

74. Pretorius, J.C.; Magama, S.; Zietsman, P.C. Purification and identification of antibacterial compounds from *Euclea crispa* subsp. *crispa* (Ebenaceae) leaves. *S. Afr. J. Bot.* **2003**, *69*, 579–586. [[CrossRef](#)]
75. Funayama, S.; Komiyama, K.; Miyaichi, Y.; Tomimiri, T.; Nozoe, S. Cytocidal and antimicrobial activities of flavonoids. *Nat. Med.* **1995**, *49*, 322–328.
76. Makati, A.C.; Ananda, A.N.; Putri, J.A.; Amellia, S.F.; Setiawan, B. Molecular docking of ethanol extracts of katuk leaf (*Sauropus androgynus*) on functional proteins of severe acute respiratory syndrome coronavirus 2. *S. Afr. J. Bot.* **2022**, *149*, 1–5. [[CrossRef](#)]
77. Novo Belchor, M.; Hessel Gaeta, H.; Fabri Bittencourt Rodrigues, C.; Ramos da Cruz Costa, C.; de Oliveira Toyama, D.; Domingues Passero, L.F.; Dalastra Laurenti, M.; Hikari Toyama, M. Evaluation of rhamnetin as an inhibitor of the pharmacological effect of secretory phospholipase A2. *Molecules* **2017**, *22*, 1441. [[CrossRef](#)] [[PubMed](#)]
78. Nawrot, J.; Budzianowski, J.; Nowak, G.; Micek, I.; Budzianowska, A.; Gornowicz-Porowska, J. Biologically active compounds in *Stizolophus balsamita* inflorescences: Isolation, phytochemical characterization and effects on the skin biophysical parameters. *Int. J. Mol. Sci.* **2021**, *22*, 4428. [[CrossRef](#)] [[PubMed](#)]

**Disclaimer/Publisher’s Note:** The statements, opinions and data contained in all publications are solely those of the individual author(s) and contributor(s) and not of MDPI and/or the editor(s). MDPI and/or the editor(s) disclaim responsibility for any injury to people or property resulting from any ideas, methods, instructions or products referred to in the content.